

# Puerarin Enhances the Anti-Tumor Effect of Cisplatin on Drug-Resistant A549 Cancer in vivo and in vitro Through Activation of the Wnt Signaling Pathway

This article was published in the following Dove Press journal:  
*Cancer Management and Research*

Ping Huang  
Shi-Xia Du

Department of Respiratory, Caoxian  
People's Hospital, Heze 274400,  
Shandong, People's Republic of China

**Objective:** The effect of PUE on enhancing the anti-cancerous efficacy of DDP on drug-resistant A549/DDP cancer and the underlying mechanisms were thoroughly investigated.

**Materials and Methods:** The cytotoxicity of PUE, DDP, and PUE + DDP to A549 cells and A549/DDP cells, respectively, is determined by cell apoptosis experiments. Anti-proliferation effect of PUE, DDP, and PUE + DDP on A549 cells and A549/DDP cells is evaluated by the cell cloning assay. Qualitative and quantitative analysis of the levels of PUE, DDP, and PUE + DDP of cell proliferation-related genes and proteins expressions in A549/DDP cells are determined by Western blot assay. The levels of VEGF in A549/DDP cells after different treatment strategies are determined by ELISA assay. Qualitative and quantitative determination of VEGF expression in tumor tissues are done by immunohistochemical staining.

**Results:** In vitro cellular experiments revealed that co-incubation of A549/DDP cells with PUE and DDP led to a dramatically decreased cell viability and cell survival rate compared with the cells only treated by DDP. Such a stimulating effect of PUE on DDP was further confirmed in vivo with results shown that the A549/DDP cancer-bearing mice treated by combination therapy achieved the lowest tumor growth rate and longest survival time.

**Conclusion:** Taking these results together, we can draw the conclusion that the PUE enhances the anti-tumor effect of DDP on the drug-resistant A549 cancer in vivo and in vitro through activation of the Wnt signaling pathway.

**Keywords:** puerarin, anti-tumor effect, cisplatin, drug-resistant, A549 cancer

## Introduction

Lung cancer is the most common malignant tumor and the leading cause of cancer-related deaths in clinic, with the 2018 Global Cancer Statistical reported that its incidence and mortality rank first among the malignant tumors.<sup>1</sup> More importantly, approximately 75–80% of all lung cancers were comprised of the non-small cell lung cancer (NSCLC).<sup>2</sup> Although the patients with early stage of NSCLC can be cured by surgical resection, more than 70% of patients are found to be a late stage of NSCLC which is characterized by local invasion or distant metastasis and inoperable.<sup>3</sup>

Despite the development of numerous chemotherapy regimens, platinum agents, such as the cisplatin (DDP), still represent a reference standard for the first-line

Correspondence: Ping Huang  
Department of Respiratory, Caoxian  
People's Hospital, Heze 274400,  
Shandong, People's Republic of China  
Tel +86 530 3490866  
Email huangpinghp0530@126.com

chemotherapy of NSCLC.<sup>4</sup> Unfortunately, the emergence of inherent or acquired clinical resistance of NSCLC cells to platinum agents dramatically impaired the final treatment efficacy.<sup>5</sup> Although the previous study revealed that chemotherapy resistance could be potentially defeated by increasing the dose of chemotherapeutic agents, the patients are always suffering from the life-threatening adverse reaction or side effects.<sup>6</sup> Exploration of novel and efficient strategies to enhance the efficacy of therapeutic intervention on DDP-resistant NSCLC is urgently needed.

Puerarin (PEU), one of the main effective components of *Pueraria Lobata*, has been characterized by owning many pharmacological effects, including slowing down heart rate, lowering blood pressure, anti-inflammatory, and regulating cellular activity.<sup>7-9</sup> Previous studies demonstrated that PEU is capable of inducing apoptosis of many types of drug-resistant-cancers.<sup>10-12</sup> However, the underlying mechanisms of PEU inhibit the growth of malignant cancers are not thoroughly investigated.

In the present study, we established a novel combination therapy strategy of PUE and DDP to combating the DDP-resistance of NSCLC. Subsequently, the effect of PUE on enhancing the anti-cancerous efficacy of DDP on the A549/DDP cancer cells and tumor-bearing mice. Additionally, the underlying mechanisms of such combination therapy of A549/DDP cancer were further thoroughly explored.

## Materials and Methods

The Puerarin and DDP were purchased from Shanghai Aladdin biochemical Technology Co., Ltd. DMSO was obtained from Beijing Solaibao Technology Co., Ltd. RPMI 1640 medium, fetal bovine serum and Trizol™ kits were purchased from Gibco. The CCK-8 kits were obtained from Dojindo. RIPA lysate and ECL kit were purchased from Shanghai Yisheng Biotechnology Co., Ltd. The ELISA kits for human Wnt3a and VEGF proteins were purchased from Wuhan Huamei Biological Engineering Co., Ltd. and antibodies used in the Western blot experiments were bought from Santa Cruz. The primary anti-bodies and the horseradish peroxidase (HRP)-conjugated anti-rabbit or anti-mouse secondary antibodies used here were purchased from Thermo (Shanghai, China). Other solvents were obtained from Sinopharm Chemical Reagent Co., Ltd. (Shanghai, China) and were of analytical or chromatographic grade.

## Cells and Animals

The non-small cell lung cancer cells A549 and cisplatin-resistant A549/DDP cells were purchased from Cancer Research Center of Chinese Academy of Medical Sciences. Both cells were cultured in RPMI 1640 medium containing 10% fetal bovine serum, 100 U/mL penicillin and streptomycin, and maintained under the condition of 37°C and 5% CO<sub>2</sub> (relative humidity 95%). Importantly, to ensure the A549/DDP cells were DDP-resistant, the A549/DDP cells were co-incubated with 0.1M DDP for 1 week before cellular experiments. The specific pathogen-free male BALB/c nude mice (20 ± 2 g) were purchased from the BK Lab Animal Ltd. (Shanghai, China) and raised at 25 ± 1°C with free access to food and water. The animal study protocol was approved by the ethics committee of China Japan Union Hospital of Jilin University (Changchun, China), and performed in accordance with the National Institutes of Health (NIH) guide for the care and use of laboratory animals.

## Cell Grouping

For cell experiments, the A549/DDP cells were respectively treated as follows: (1) Control group: A549/DDP cells only treated by the cell culture medium; (2) PUE group: A549/DDP cells received the monotherapy of PUE (120 µg/mL); (3) A549/DDP cells received the monotherapy of DDP (40 µg/mL); (4) A549/DDP cells received the combination therapy of PUE and DDP (120 µg/mL+40 µg/mL). The cells in each group were co-incubated with drugs or medium for 48 h under the condition of 37°C and 5% CO<sub>2</sub>.

## CCK-8 Experiments

The cells in logarithmic growth phase were digested with 0.25% trypsin to prepare cell suspension. After centrifugation, the old culture medium was discarded, the fresh culture medium was added to adjust the cell concentration to 5 × 10<sup>4</sup> mL, and the cell suspension was inoculated to 96 well culture plates according to 100 µl/well. The cells were divided into four groups and treated as above. After 48 h of incubation, 10 µL CCK-8 solution was added into each well of the plates followed by the detection of absorbance (OD values) at 450 nm.

## Cell Apoptosis Assay

The digestion and inoculation of A549/DDP cells were the same as above. Then the cells were divided into four groups and treated as above. After incubation for 24 h,

the cells were trypsinized and collected by centrifugation at 1000 g for 5 min. Then the obtained cell pellets were re-suspended in 200  $\mu$ L binding buffer for double staining with Annexin V-FITC (5  $\mu$ L) and PI (10  $\mu$ L). Finally, the cell survival rate was evaluated by the flow cytometer (FACSCalibur, BD, USA).

### Cell Cloning Experiments

The A549/DDP cells were incubated with drugs according to cell grouping mentioned above. After 24 h of incubation, the treated cells were digested with trypsin, and then inoculated into 6-well culture plate according to  $2 \times 10^3$ /well. Two weeks later, the number of clones was determined by staining with methylene blue (0.04%).

### Cell Migration Assay

A549/DDP cells in logarithmic growth phase were seeded into 6-well plates at the density of  $8 \times 10^5$  cells/well. Then the cells were allowed to grow for 24h to form a monolayer cells. After that, a “one” zigzag scratch along the bottom of the culture hole was created by a plastic pipette tip. To evaluate the invasion inhibition effect of PEU or DDP, the A549/DDP cells were divided into four groups and then treated as the cell grouping assay. Thereafter, the cells were observed every 2 hours until the scratches were filled with cells and the time required for the cells to cross the river was also recorded.

### In vivo Anti-Tumor Effect

To evaluate the anti-tumor effect in vivo, the A549/DDP tumor-bearing mice were established first. In brief, Sixty BALB/c nude mice were subcutaneously injected on the right armpit with A549/DDP cell suspensions ( $1 \times 10^7$ /100 mL) and then raised under the standard conditions. Two weeks later, the tumor-bearing mice were randomly grouped ( $n=10$ ) and treated with PUE (60 mg/kg), DDP (10 mg/kg), and combination of PUE and DDP (60 mg/kg +10 mg/kg). Of great importance, the mice injected with equivalent volume of Saline were used as the control group. After the therapy strategies were repeated every 2 days in 1 week, the survival time of mice in each group was carefully observed and recorded. For determination of tumor growth inhibition, twenty tumor-bearing mice were randomly grouped ( $n=5$ ) and treated as above. Twenty-one days after a week of treatment, all the mice were sacrificed with tumor tissues in each group were collected for qualitative and quantitative analysis. The tumor volumes were calculated by the formula as following: volume = length  $\times$

width<sup>2</sup>/2. Additionally, the obtained tumor tissues were further subjected to immunohistochemical staining for detection of VEGF expression, and Western blot analysis.

### Western Blot Experimental Method

The drug-treated A549/DDP cells or DDP non-resistant A549 cells were collected for lysing by RIPA lysis buffer (100–200  $\mu$ L lysate, 5 min) on ice bath. Then the protein samples were achieved by centrifuging the mixture for 30 min at 14000 rpm under 4°C. After that, the concentration of protein samples was determined by BCA protein quantitative kit (Pierce, Rockford, IL, USA) before they were separated by 10% SDS-polyacrylamide gel electrophoresis (SDS-PAGE, 150V, 90 mins). Then, all the samples were transferred into polyvinylidene difluoride membrane (PVDF, Millipore, Billerica, MA) followed by blocking with 5% non-fat dried milk 1 h under room temperature. For detection of proteins, various primary antibodies were introduced and incubated with samples at 4°C for 1 h before added with various corresponding secondary antibodies. After an overnight of incubation, the horseradish peroxidase-labeled IgG (1:1000, LK2003L, Sungene Biotech Co., Ltd, China) was added and incubated with samples for 1 h. Finally, the expressions of various proteins were determined by the Bio-Rad microscopic imaging system (Bio-Rad, Hercules, CA). For detection of proteins in vivo, the obtained tumor tissues were subjected to homogenate firstly. Then the levels of various proteins were detected using the methods as above.

### ELISA Experiments

For quantitative analysis of the expression of various proteins in A549/DDP cells or tumor tissues after treatment, the ELISA experiments were conducted. In brief, the A549/DDP cells or DDP non-resistant A549 cells after various treatments were collected and washed three times. Then the detection of proteins was performed according to the instructions of ELISA kit. For determination of proteins in tumor tissues, the obtained tumor tissues were subjected to homogenate firstly followed by detection using the same methods.

### Immunohistochemistry (IHC) Assay and Histological Observation

All the collected tumor tissues were washed three times with saline and subsequently fixed in 4% formalin for 1 h. Then

the tumor tissues were embedded in paraffin for preparation of 4  $\mu\text{m}$  thick tumor slides. For protein detection, all tumor slides were incubated with 10 mM citrate buffer at 100°C for 10 min before incubated with anti-VEGF (1: 25, Abcam, ab18197) for overnight at 4°C. Thereafter, anti-rabbit secondary antibody (Abcam, ab150077) was added and incubated with the tumor slides for 2 h. Finally, the results were obtained through the optical microscope. The obtained kidney tissues were fixed with formalin followed by immersion in paraffin. Then the histological assessment of toxicity of puerarin, cisplatin, and puerarin + cisplatin to kidney tissues was determined using the hematoxylin and eosin (H&E) staining.

## Statistical Analysis

SPSS18.0 software was applied to perform the statistical analysis. The data were presented by mean  $\pm$  standard (mean  $\pm$ SD). The *t*-test was conducted for comparison between two groups. Statistical significance was defined as  $p < 0.05$ .

## Results

### PUE Signally Enhanced the Inhibitory Effect of DDP on the Viability of A549/DDP Cells

As shown in Figure 1A and B, characterization of the chemical structure of PUE and DDP. As shown in Figure 1C and D, both PUE and DDP inhibited the growth of A549/DDP cells and the DDP non-resistant cells in a concentration-dependent manner. Moreover, the anti-growth effect of PUE and DDP on the DDP non-resistant A549 cells was significantly stronger than that of A549/DDP cells. These results indicated that the DDP non-resistant A549 cells were more sensitive to the treatment of PUE or DDP. The combination therapy effect of PUE and DDP was further investigated. As demonstrated in Figure 1E and F, the cells received the combination therapy of PUE and DDP exhibited an obvious slower growth rate compared with the cells only treated by DDP. Such results suggested that the incubation of A549/DDP cells with PUE could significantly improve the cytotoxicity of DDP.

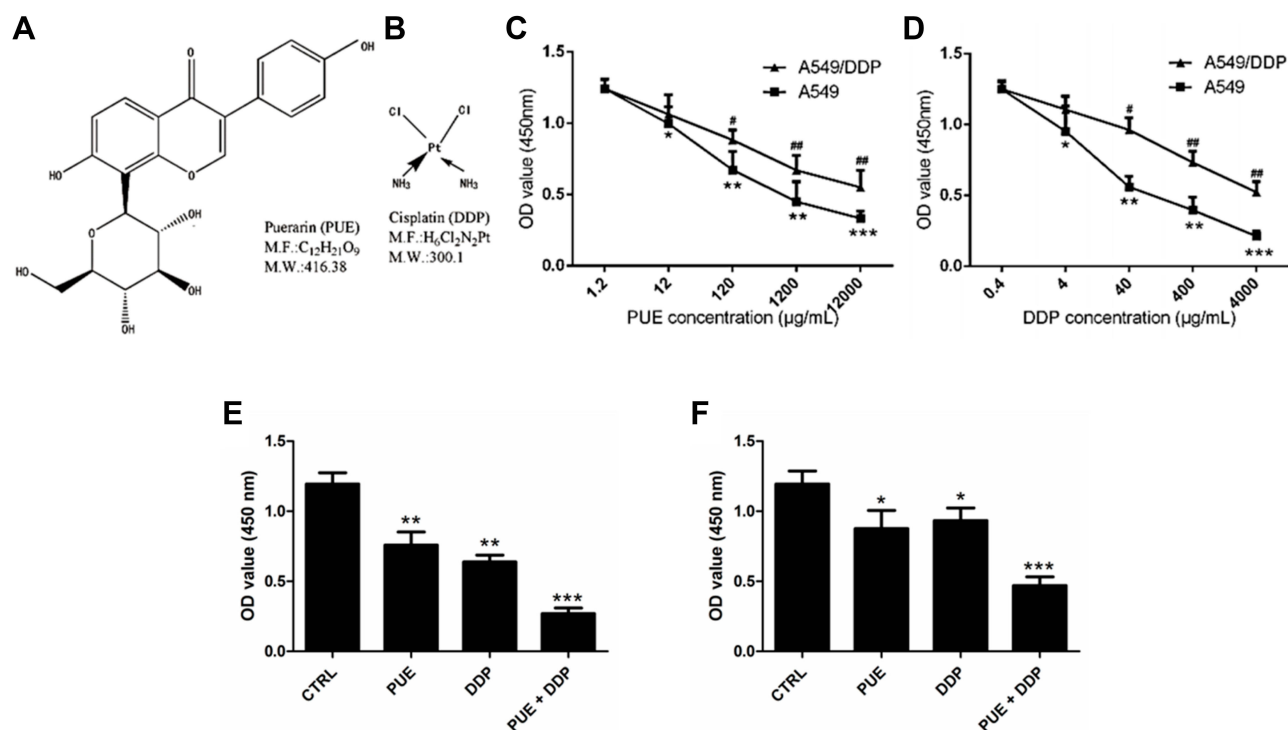


**Figure 1** Evaluation of the effect of PUE and DDP on cell growth of A549 cells and A549/DDP cells, respectively. (A) Characterization of the chemical structure of PUE. (B) Characterization of the chemical structure of DDP. (C) Cell viability of A549/DDP cells and A549 cells post treatment of PUE. (D) Cell viability of A549/DDP cells and A549 cells post treatment of DDP. (E) Effect of combination therapy of PUE and DDP on the viability of A549 cells compared with the monotherapy. (F) Effect of combination therapy of PUE and DDP on the viability of A549/DDP cells compared with the monotherapy. \* $p < 0.05$ , \*\* $p < 0.01$ , \*\*\* $p < 0.001$ , # $p < 0.05$ , ## $p < 0.01$ , compared with controls.

## PUE Dramatically Improved the Effect of DDP on Inducing Apoptosis and Anti-Proliferation of A549/DDP Cells

As shown in **Figure 2A**, both the PUE and DDP exhibited obvious higher cytotoxicity to the A549 cell than the DDP-resistant A549/DDP cells. Additionally, the effect of combinational therapy of PUE and DDP was further investigated on the above two kinds of cells. Result demonstrated that the combinational treatment of PUE and DDP displayed the highest ability of cell apoptosis inducing. Most importantly, the insufficient toxicity of DDP to the A549/DDP cells was significantly enhanced after co-treating the cells with PUE, indicating that the DDP-resistance of A549/DDP cells could be overcome by the combination therapy of PUE and DDP.

For further confirmation of the combination effect of PUE and DDP on A549/DDP cells, the cell cloning assay was conducted. As demonstrated in **Figure 2B**, the average number of A549/DDP cells in the group of PUE+DDP was the lowest with a value of  $80.68 \pm 11.79$ , while other groups were  $183.21 \pm 21.70$  in control group,  $148.33 \pm 11.79$  in PUE group, and  $145.49 \pm 13.69$  in DDP group, respectively.

To evaluate the combinational effect of PUE and DDP at molecular level, the cancer cell proliferation favorable proteins Ki67 and PCNA were determined by Western blot experiments. As results shown in **Figure 2C** and **D**, the levels of Ki67 and PCNA in A549/DDP cells could dramatically down-regulated by treating with PUE or DDP. Interestingly, the expression of Ki67 and PCNA in A549/DDP cells that only treated by PUE or DDP is markedly higher than the cells treated by combination of PUE and DDP.

## Combination Therapy of PUE and DDP Significantly Inhibited the Migration of A549/DDP Cells

To evaluate the lateral migration ability of A549/DDP cells after various treatments, the wound healing assay was performed. As shown in **Figure 3A**, after 24 h of incubation, the cells untreated with drugs (control group) exhibited the strongest migration ability since they achieved the best wound healing, with a wound healing rate of nearly 100%. In contrast, the migration ability of A549/DDP cells was significantly down-regulated after

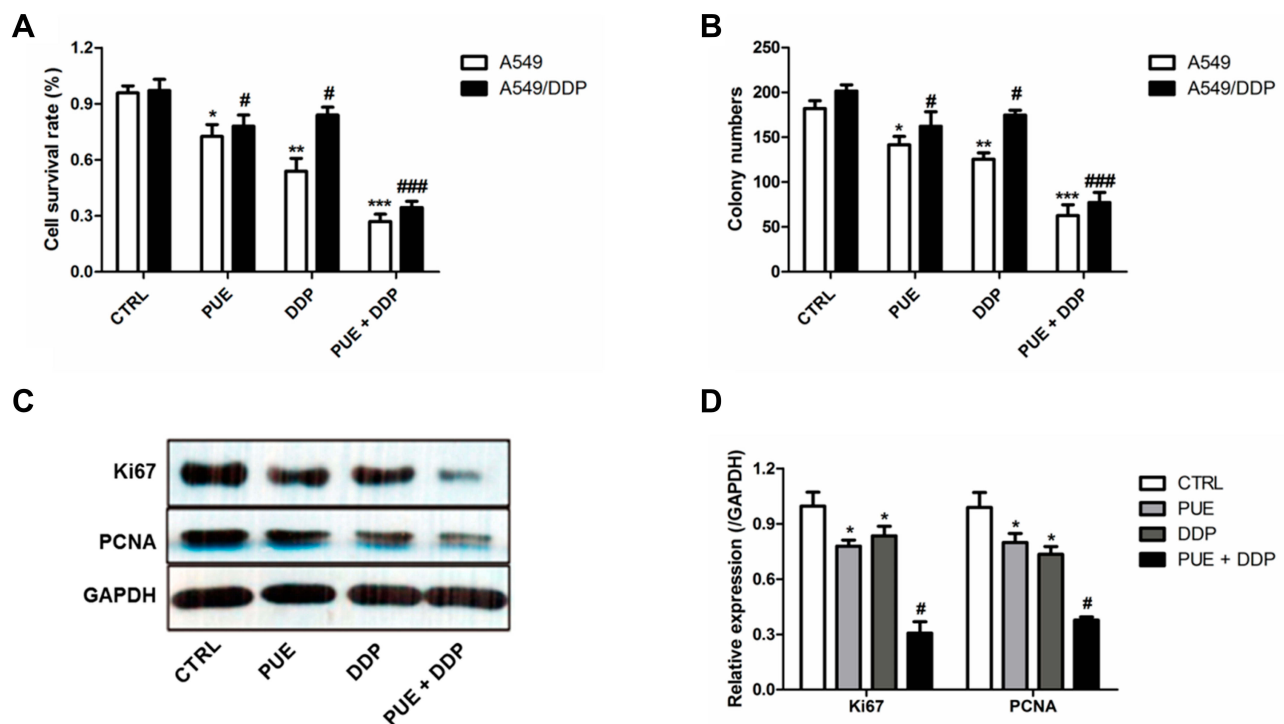


**Figure 2** Combination effect of PUE and DDP on inducing apoptosis and anti-proliferation of A549/DDP cells compared with the monotherapy of PUE or DDP. **(A)** Determination of the cytotoxicity of PUE, DDP, and PUE + DDP to A549 cells and A549/DDP cells, respectively, by cell apoptosis experiments. **(B)** Anti-proliferation effect of PUE, DDP, and PUE + DDP on A549 cells and A549/DDP cells evaluated by the cell cloning assay. Qualitative **(C)** and quantitative **(D)** analysis of the effect of PUE, DDP, and PUE + DDP on the regulation of cell proliferation-related genes expressions in A549/DDP cells by Western blot assay. \* $p < 0.05$ , \*\* $p < 0.01$ , \*\*\* $p < 0.001$ , # $p < 0.05$ , ### $p < 0.05$ , compared with controls.

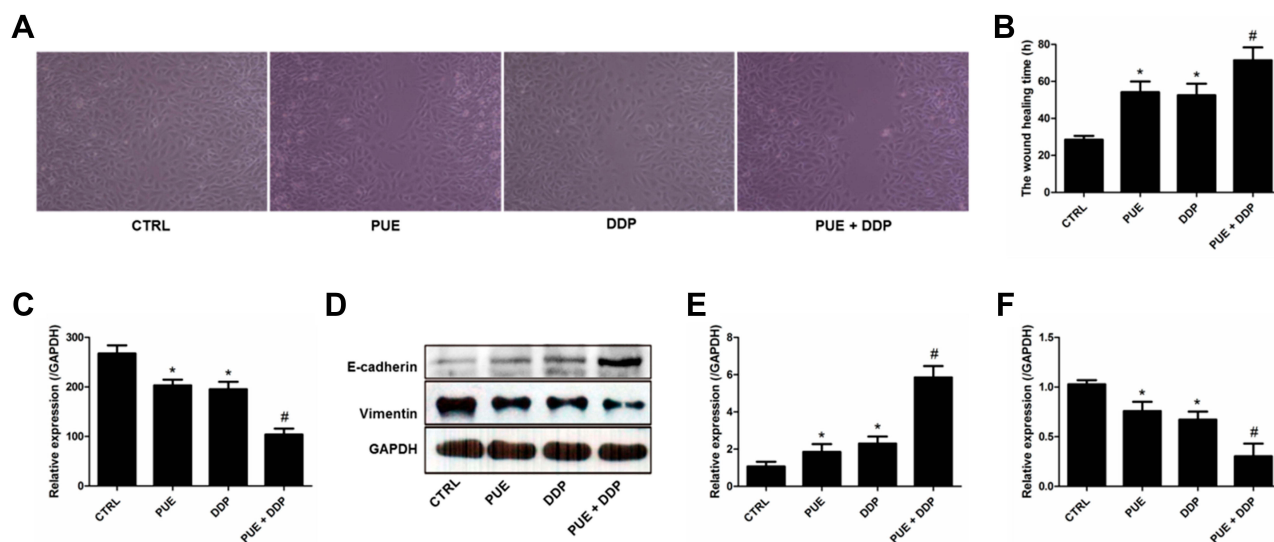


**Figure 3** Migration of A549/DDP cells inhibited by various treatments and investigation of the underlying molecular mechanism. **(A)** Wound healing images after scratch incubation with drug-free medium (Control group), PUE (120  $\mu\text{g}/\text{mL}$ ), DDP (40  $\mu\text{g}/\text{mL}$ ), and PUE and DDP (120  $\mu\text{g}/\text{mL}$ +40  $\mu\text{g}/\text{mL}$ ). **(B)** Quantitative analysis of the inhibition effect of various formulations on the migration of A549/DDP cells. **(C)** Determination of the levels of VEGF in A549/DDP cells after different treatment strategies by ELISA assay. **(D)** Qualitative evaluation of the levels of E-cadherin and Vimentin in A549/DDP cells after different treatment strategies by Western blot experiments. **(E)** Quantitative analysis of the expression of E-cadherin post various treatments. **(F)** Quantitative analysis of the expression of Vimentin post various treatments. \* $p < 0.05$ , compared with controls. # $p < 0.05$  compared with the cells only treated by DDP.

incubated with PUE or DDP. Moreover, the A549/DDP cells in the group treated by combination therapy of PUE and DDP exhibited the worst migration, with only a wound healing rate of 18%. We further investigated the wound healing time after treated the A549/DDP cells with various strategies. As results revealed that the cells in control group displayed the most rapid wound healing speed, with a crossing time of  $30.05 \pm 3.12$  h. However, the wound healing speed of A549/DDP cells was dramatically inhibited by incubation with PUE ( $52.75 \pm 4.99$  h) or DDP ( $50.51 \pm 3.37$  h). Additionally, co-incubation with cells with PUE+DDP displayed the strongest inhibition effect on the migration speed of A549/DDP cells since it achieved the longest crossing time ( $67.82 \pm 5.26$  h) (Figure 3B).

Molecular mechanism studies revealed that the expression of E-cadherin, an intracellular adhesion-related protein, in A549/DDP cells was signally up-regulated after treated by PEU or DDP (Figure 3D and E). In contrast, the levels of VEGF (Figure 3C) and Vimentin (Figure 3D and F), which are the key proteins promote cancer cell invasion, were dramatically decreased after incubated cells with PEU or DDP. Of great importance, the cells treated by PEU+DDP exhibited the highest expression levels for E-cadherin and the lowest expression levels for VEGF and Vimentin.

## PUE Enhances the Effect of DDP on the Inhibition of Wnt/ $\beta$ -Catenin Pathway in A549/DDP Cells

As the results of ELISA test shown in Figure 4A revealed that additional treatment of the DDP-treated A549/DDP cells with PEU further signally down-regulated the expression levels of Wnt3a. Quantitative analysis exhibited that the concentration of Wnt3a in the control group was  $372.54 \pm 33.07$  pg/mL. After the cells were, respectively, treated by PEU, DDP, and PEU+DDP, the concentrations were decreased to  $293.89 \pm 22.64$  pg/mL,  $286.74 \pm 25.33$  pg/mL, and  $170.38 \pm 20.25$  pg/mL, respectively.

For further confirmation, the Western blot experiments were performed to determine the levels of Wnt/ $\beta$ -catenin-related proteins in A549/DDP cells. As shown in Figure 4B and C, when compared with the cells in control group, the cells treated with DDP displayed an obvious decreased expression of  $\beta$ -catenin, c-Myc, Cyclin D1, MMP3, and MMP9. More importantly, co-treating A549/DDP cells with PEU and DDP further significantly enhanced the inhibition ability of DDP on the expression of these Wnt/ $\beta$ -catenin-related proteins. These results together indicated that the PUE dramatically enhances the effect of DDP on inhibition of A549/DDP cell growth, proliferation, and migration through silencing the Wnt/ $\beta$ -catenin pathway.

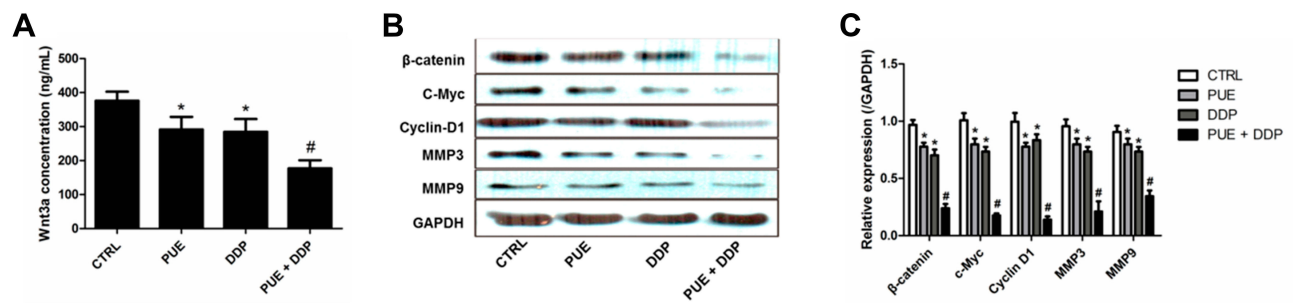


**Figure 4** Evaluation of the underlying mechanisms of PUE enhances the effect of DDP on inhibition of A549/DDP cell growth, proliferation, and migration. **(A)** Determination of the levels of Wnt3a in A549/DDP cells by ELISA test after treated by various strategies. Qualitative **(B)** and quantitative **(C)** evaluation of the Wnt/ $\beta$ -catenin-related proteins, including  $\beta$ -catenin, c-Myc, Cyclin D1, MMP3, and MMP9, in A549/DDP cells after treatment by Western blot assay. \* $p < 0.05$ , compared with controls. # $p < 0.05$  compared with the cells only treated by DDP.

## PEU Significantly Improve the Anti-Tumor Effect of DDP While Protecting Kidney from Cisplatin Toxicity

The anti-tumor effect of combination of PEU and DDP was finally evaluated in the A549/DDP tumor-bearing mice. Results shown in Figure 5A confirmed that the mice treated with PEU+DDP achieved the longest survival time, indicating a superior tumor growth inhibition effect for the combination therapy strategy. For further confirmation, tumor growth inhibition assay was conducted. As shown in Figure 5B, the mice treated with DDP exhibited an obvious smaller tumor volume compared with the control group. Importantly, co-treating the mice with PEU and DDP further markedly decreased the tumor volumes. Such results were further demonstrated by the quantitative analysis results, with the tumor volumes in control group, PUE group, DDP group and PUE+DDP group were  $976.2 \pm 93.4$ ,  $671.5 \pm 78.8$ ,  $636.1 \pm 80.9$  and  $348.6 \pm 62.3 \text{ mm}^3$ , respectively (Figure 5C).

Additionally, immunohistochemical staining experiments were performed to evaluate the expression of VEGF in tumor tissues post various treatments. Results in Figure 5D and E displayed a similar trend to the cellular assays, with the tumor tissues treated by PUE+DDP exhibited the lowest levels of VEGF. Moreover, the results of Western blot revealed that the expressions of Ki67 and PCNA in the DDP-treated tumor tissues could be further signally down-regulated by co-treating with PEU (Figure 5F and G). Besides, the Wnt/ $\beta$ -catenin pathway-related proteins, including  $\beta$ -catenin, c-Myc, Cyclin D1, MMP3, and MMP9, in tumor tissues were also determined. As shown in Figure 5H and I, when compared with the control group, the levels of proteins in the tumor tissues of

mice treated by DDP were dramatically decreased. More importantly, the expression of these proteins in the DDP-treated mice could be further down-regulated after given with the combination therapy of PEU and DDP.

The toxicity of puerarin, cisplatin, and puerarin + cisplatin to kidney of mice was further investigated. As shown in Figure 5J and K, the PUE exhibited negligible toxicity to kidney tissues of mice compared with the control group. However, the DDP-treated mice displayed the highest damage rate compared with others. Interestingly, the mice in the group of puerarin + cisplatin exhibited obvious lower damage rate of kidney tissues than the DDP group. Such results indicated that the puerarin was able of attenuating the cisplatin-induced nephrotoxicity.

## Discussion

Although the rapid development of therapeutic strategies, the prognosis for patients with advanced non-small-cell lung cancer (NSCLC) remains poor mainly due to the rapid progress chemotherapy-resistance of such tumor.<sup>13</sup> At present, the platinum-based chemotherapy is the most common and reference standard treatment for NSCLC.<sup>14</sup> However, the final treatment efficacy is inadequate due to the emergence of inherent or acquired clinical resistance of NSCLC cells to platinum agents.<sup>5</sup> As the previous study pointed out, 5-year survival rate of patients with NSCLC treated by DDP was only 4% to 17%.<sup>15</sup>

PEU has been reported with anti-tumor activity in many kinds of many types of drug-resistant-cancers.<sup>10,11</sup> Based on this, we established the combination therapy strategy of PUEplus DDP to combating the DDP-resistance of NSCLC. In our studies, cell viability assay confirmed that treating A549/DDP cells with PUE+DDP resulted in lower cell viability compared with the cells

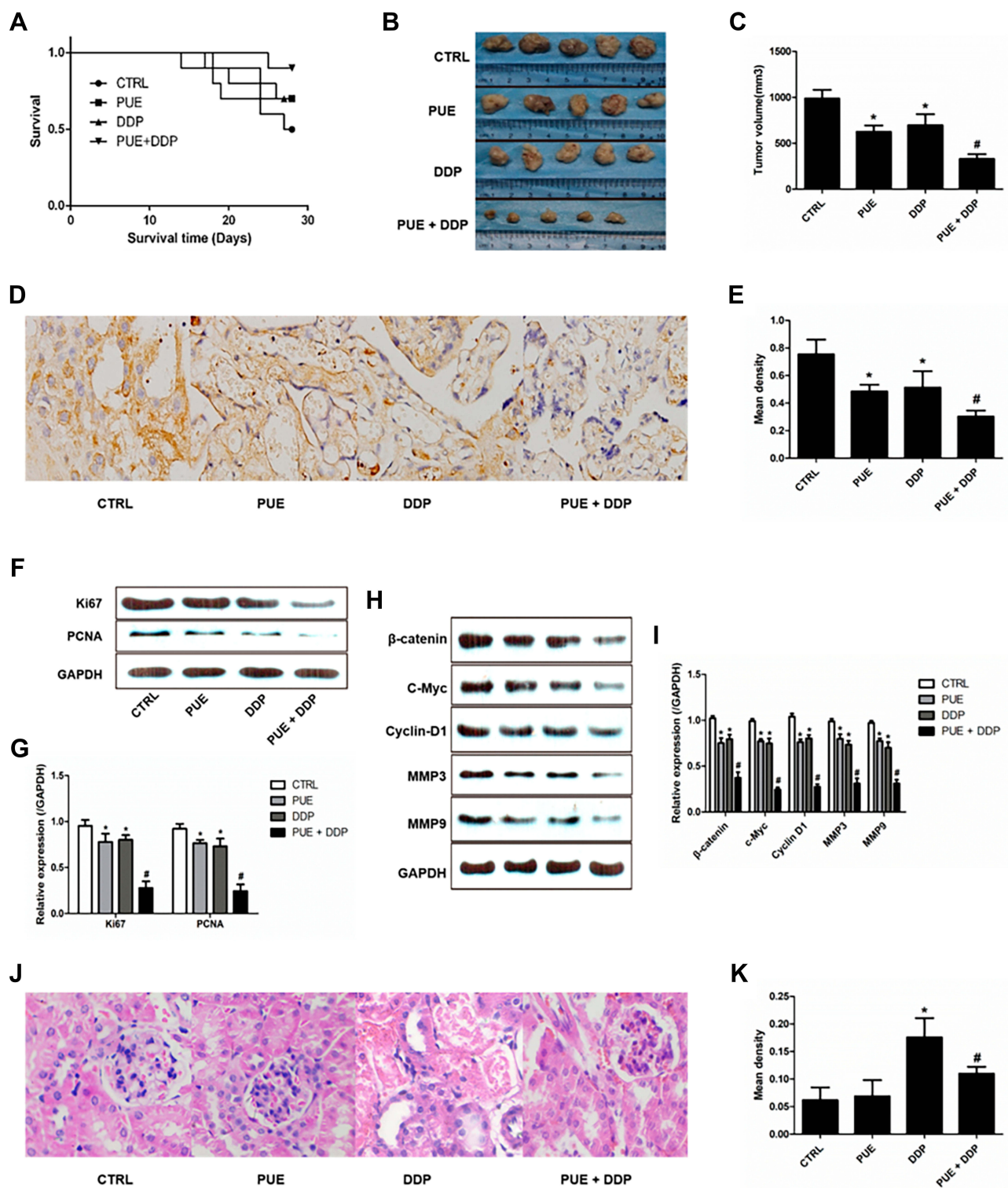


**Figure 5** Anti-tumor effect of various treatment strategies in the A549/DDP tumor-bearing mice. **(A)** Kaplan-Meier survival curves of A549/DDP tumor-bearing mice after treated by PUE (60 mg/kg), DDP (10 mg/kg), and combination of PUE and DDP (60 mg/kg+10 mg/kg) ( $n=10$ ). Qualitative images **(B)** and quantitative analysis **(C)** of tumor volumes after the treatment of various formulations ( $n=5$ ). Qualitative **(D)** and quantitative **(E)** determination of VEGF expression in tumor tissues by immunohistochemical staining. **(F and G)** Evaluation of the expression levels of cell apoptosis-related proteins (Ki67 and PCNA) after various treatments. **(H and I)** Evaluation of the expression levels of the Wnt/ $\beta$ -catenin pathway-related proteins ( $\beta$ -catenin, c-Myc, Cyclin D1, MMP3, and MMP9) after various treatments. Qualitative **(J)** and quantitative **(K)** determination of the damage rate of kidney tissues of mice after respectively treated by puerarin, cisplatin, and puerarin + cisplatin. \* $p < 0.05$ , compared with controls. # $p < 0.05$  compared with the cells only treated by DDP.

only treated by DDP. Moreover, the cells received the combination therapy of PUE and DDP exhibited an obvious lower cell proliferation rate compared with the cells treated by monotherapy of DDP. Such results were mainly derived from that PUE significantly enhanced the sensitivity of A549/DDP cells to the treatment of DDP. However, the underlying mechanisms were not thoroughly investigated.

Transformation of epithelial cells into stroma (EMT) refers to the process of transforming epithelial cells into stroma cells, which is closely related to the proliferation and migration of tumor cells.<sup>16</sup> In general, the tumor progress-related EMT is often accompanied by decreasing the expression level of E-cadherin and transformation of cytokeratin cytoskeleton into vimentin-based cytoskeleton.<sup>16,17</sup> In this case, EMT has been considered to be one of the important factors that provoke tumor drug-resistance and the occurrence of EMT has been observed in many kinds of drug-resistant cancer cells.<sup>18–20</sup> In the present study, results of Western blot revealed that the expression of E-cadherin in A549/DDP cells was dramatically down-regulated after co-treatment with PUE and DDP. In contrast, the level of Vimentin was markedly increased after the combination therapy of PUE and DDP.

Additionally, previous studies revealed that the expression of VEGF plays a significant role in the promotion of many kinds of tumor progress, including the NSCLC.<sup>21</sup> The mechanism of VEGF promotes tumor progress is mainly lies in that VEGF is a favorable molecular regulator that participates in proliferation, differentiation, and migration of many cancer cells.<sup>21</sup> Our studies revealed that the treatment of A549/DDP cells with PUE could dramatically down-regulate the expression levels of VEGF. Besides, the levels of VEGF in DDP-treated A549/DDP cells were further decreased after additional treatment of PUE.

Wnt/ $\beta$ -catenin pathway, representing one of the most important signaling pathway, is always involved in many biological processes, such as proliferation, differentiation, apoptosis and migration of cells.<sup>22</sup> After binding to the curly protein on the cell membrane, the endogenous ligand of Wnt (such as Wnt3a) can inhibit the formation of  $\beta$ -catenin degradation complex Axin/APC/GSK3  $\beta$ , thus inhibiting the degradation of  $\beta$ -catenin.<sup>23</sup> Then the  $\beta$ -catenin was inserted into the nucleus to regulate the downstream target genes, such as cell cycle protein C-Myc, Cyclin D1 and proteolytic enzymes MMP3 and MMP9.<sup>24</sup> Accumulating evidences demonstrated that aberrant activation of Wnt/ $\beta$ -catenin pathway plays an important role

in the occurrence and development of many kinds of malignant tumors.<sup>25–29</sup> PUE has been reported with the ability of regulating the Wnt/ $\beta$ -catenin pathway and therefore holds great potential in anti-tumor progress.<sup>30</sup> Our study confirmed that treating the A549/DDP cells with PUE significantly decreased the levels of Wnt/ $\beta$ -catenin pathway-related proteins, including  $\beta$ -catenin, c-Myc, Cyclin D1, MMP3, and MMP9. Importantly, such effect of PUE on silencing Wnt/ $\beta$ -catenin pathway signally enhanced the inhibition effect of DDP on the growth, proliferation, and migration of A549/DDP cells.

Based on the above results, we finally investigated the anti-tumor effect of PUE+DDP on A549/DDP cells-tumor bearing mice. Similar to the in vitro cellular experiments, PUE significantly improved the inhibition effect of DDP on the growth of A549/DDP tumors, with the mice treated with PUE+DDP achieved the longest survival time. Besides, the tumor tissues treated by combination therapy of PUE and DDP exhibited the lowest levels of VEGF and Wnt/ $\beta$ -catenin pathway-related proteins. Additionally, a previous study pointed out that puerarin has antitumor effect against chromosome breakage or loss and DNA damage.<sup>31</sup> Moreover, it was also reported that puerarin exhibited no inhibitory influence on the antitumor effects of cisplatin while protecting kidney from cisplatin toxicity.<sup>32</sup> In our study, we demonstrated that the high damage rate of kidney tissues of the cisplatin-treated mice could be dramatically alleviated by co-treated with puerarin. Taking these results together, it could be concluded that the puerarin significantly enhanced the anti-tumor effect of cisplatin while protecting kidney from cisplatin toxicity.

## Conclusion

PUE is able of inhibiting the proliferation and migration of human lung cancer cells by inhibiting the activation of Wnt/ $\beta$ -catenin signaling pathway and affecting the expression of cyclins and proteolytic enzymes. It was confirmed that PUE could significantly enhance the anti-tumor effect of DDP on A549/DDP cells in vivo and in vitro. Therefore, the results of this study indicated that the PUE holds great potential in treating with advanced lung cancer, and provides a promising treatment strategy for reverse the chemotherapy resistance of NSCLC.

## Disclosure

The authors declare no competing financial or non-financial interests.

## References

- Bray F, Ferlay J, Soerjomataram I, Siegel RL, Torre LA, Jemal A. Global cancer statistics 2018: GLOBOCAN estimates of incidence and mortality worldwide for 36 cancers in 185 countries. *CA Cancer J Clin*. 2018;68:394–424. doi:10.3322/caac.21492
- Chen W, Zheng R, Baade PD, et al. Cancer statistics in China, 2015. *CA Cancer J Clin*. 2016;66:115–132. doi:10.3322/caac.21338
- Mokhles S, Nuyttens JJ, Maat AP, et al. Survival and treatment of non-small cell lung cancer stage I-II treated surgically or with stereotactic body radiotherapy: patient and tumor-specific factors affect the prognosis. *Ann Surg Oncol*. 2015;22:316–323. doi:10.1245/s10434-014-3860-x
- Capelletto E, Novello S, Scagliotti GV. First-line therapeutic options for advanced non-small-cell lung cancer in the molecular medicine era. *Future Oncol*. 2014;10:1081–1093. doi:10.2217/fon.13.247
- MacDonagh L, Gray SG, Breen E, et al. Lung cancer stem cells: the root of resistance. *CA Cancer Lett*. 2016;372:147–156. doi:10.1016/j.canlet.2016.01.012
- Zhou YX, Zhang H, Peng C. Puerarin: a review of pharmacological effects. *Phytother Res*. 2014;28:961–975. doi:10.1002/ptr.5083
- Ye G, Kan S, Chen J, Lu X. Puerarin in inducing apoptosis of bladder cancer cells through inhibiting SIRT1/p53 pathway. *Oncol Lett*. 2019;17:195–200. doi:10.3892/ol.2018.9600
- Liu X, Zhao W, Wang W, Lin S, Yang L. Puerarin suppresses LPS-induced breast cancer cell migration, invasion and adhesion by blockage NF- $\kappa$ B and Erk pathway. *Biomed Pharmacother*. 2017;92:429–436. doi:10.1016/j.biopha.2017.05.102
- Zhang XL, Wang BB, Mo JS. Puerarin 6"-O-xyloside possesses significant antitumor activities on colon cancer through inducing apoptosis. *Oncol Lett*. 2018;16:5557–5564. doi:10.3892/ol.2018.9364
- Hu Y, Li X, Lin L, Liang S, Yan J. Puerarin inhibits non-small cell lung cancer cell growth via the induction of apoptosis. *Oncol Rep*. 2018;39:1731–1738. doi:10.3892/or.2018.6234
- Chen T, Chen H, Wang Y, Zhang J. In vitro and in vivo antitumor activities of puerarin 6"-O-xyloside on human lung carcinoma A549 cell line via the induction of the mitochondria-mediated apoptosis pathway. *Pharm Biol*. 2016;54:1793–1799. doi:10.3109/13880209.2015.1127980
- Anukunwithaya T, Poo P, Hunsakunachai N, Rodsiri R, Malaivijitnond S, Khemawoot P. Absolute oral bioavailability and disposition kinetics of puerarin in female rats. *BMC Pharmacol Toxicol*. 2018;25:25. doi:10.1186/s40360-018-0216-3
- Tan WL, Jain A, Takano A, et al. Novel therapeutic targets on the horizon for lung cancer. *Lancet Oncol*. 2016;17:e347–e362. doi:10.1016/S1470-2045(16)30123-1
- Wakelee H, Kelly K, Edelman MJ. 50 years of progress in the systemic therapy of non-small cell lung cancer. *Am Soc Clin Oncol Educ Book*. 2014;34:177–189. doi:10.14694/EdBook\_AM.2014.34.177
- Hirsch HR, Scagliotti GV, Mulshine JL, et al. Lung cancer: current therapies and new targeted treatments. *Lancet*. 2017;389:299–311. doi:10.1016/S0140-6736(16)30958-8
- Suarez-Carmona M, Lesage J, Cataldo D, Gilles C. EMT and inflammation: inseparable actors of cancer progression. *Mol Oncol*. 2017;11:805–823. doi:10.1002/1878-0261.12095
- Tian T, Sun J, Wang J, Liu Y, Liu H. Isoliquiritigenin inhibits cell proliferation and migration through the PI3K/AKT signaling pathway in A549 lung cancer cells. *Oncol Lett*. 2018;16:6133–6139. doi:10.3892/ol.2018.9344
- Fiori ME, Di Franco S, Villanova L, Bianca P, Stassi G, De Maria R. Cancer-associated fibroblasts as abettors of tumor progression at the crossroads of EMT and therapy resistance. *Mol Cancer*. 2019;18:70. doi:10.1186/s12943-019-0994-2
- Yochum ZA, Cades J, Wang H, et al. Targeting the EMT transcription factor TWIST1 overcomes resistance to EGFR inhibitors in EGFR-mutant non-small-cell lung cancer. *Oncogene*. 2019;38:656–670. doi:10.1038/s41388-018-0482-y
- Sosa Iglesias V, Giuranno L, Dubois LJ, Theys J, Vooijs M. Drug resistance in non-small cell lung cancer: a potential for NOTCH targeting. *Front Oncol*. 2018;8:267. doi:10.3389/fonc.2018.00267
- Yang F, Qin Z, Shao C, et al. Association between VEGF gene polymorphisms and the susceptibility to lung cancer: an updated meta-analysis. *Biomed Res Int*. 2018;2018:9271215.
- Kretzschmar K, Clevers H. Wnt/ $\beta$ -catenin signaling in adult mammalian epithelial stem cells. *Dev Biol*. 2017;428:273–282. doi:10.1016/j.ydbio.2017.05.015
- Hafeez BB, Ganju A, Sikander M, et al. Ormeloxifene suppresses prostate tumor growth and metastatic phenotypes via inhibition of oncogenic  $\beta$ -catenin signaling and EMT progression. *Mol Cancer Ther*. 2017;16:2267–2280. doi:10.1158/1535-7163.MCT-17-0157
- Yu W, Li L, Zheng F, et al.  $\beta$ -catenin cooperates with CREB binding protein to promote the growth of tumor cells. *Cell Physiol Biochem*. 2017;44:467–478. doi:10.1159/000485013
- Chen Z, He J, Xing X, et al. Mn12Ac inhibits the migration, invasion and epithelial-mesenchymal transition of lung cancer cells by down-regulating the Wnt/ $\beta$ -catenin and PI3K/AKT signaling pathways. *Oncol Lett*. 2018;16:3943–3948. doi:10.3892/ol.2018.9136
- Zhang Q, Zhang B, Sun L, et al. MicroRNA-130b targets PTEN to induce resistance to cisplatin in lung cancer cells by activating Wnt/ $\beta$ -catenin pathway. *Cell Biochem Funct*. 2018;36:194–202. doi:10.1002/cbf.3331
- Che J, Yue D, Zhang B, et al. Claudin-3 inhibits lung squamous cell carcinoma cell epithelial-mesenchymal transition and invasion via suppression of the Wnt/ $\beta$ -catenin signaling pathway. *Int J Med Sci*. 2018;15:339–351. doi:10.7150/ijms.22927
- Zhang K, Wang J, Yang L, et al. Targeting histone methyltransferase G9a inhibits growth and Wnt signaling pathway by epigenetically regulating HP1 $\alpha$  and APC2 gene expression in non-small cell lung cancer. *Mol Cancer*. 2018;17:153. doi:10.1186/s12943-018-0896-8
- Han F, Liu W-B, Shi X-Y, et al. SOX30 inhibits tumor metastasis through attenuating Wnt-signaling via transcriptional and post translational regulation of  $\beta$ -catenin in lung cancer. *EBioMedicine*. 2018;31:253–266. doi:10.1016/j.ebiom.2018.04.026
- Huang GR, Wei SJ, Huang YQ, Xing W, Wang LY, Liang LL. Mechanism of combined use of vitamin D and puerarin in anti-hepatic fibrosis by regulating the Wnt/ $\beta$ -catenin signalling pathway. *World J Gastroenterol*. 2018;24:4178–4185. doi:10.3748/wjg.v24.i36.4178
- Bacanlı M, Başaran AA, Başaran N. The antioxidant, cytotoxic, and antigenotoxic effects of galangin, puerarin, and ursolic acid in mammalian cells. *Drug Chem Toxicol*. 2017;40:256–262. doi:10.1080/01480545.2016.1209680
- Ma X, Yan L, Zhu Q, Shao F. Puerarin attenuates cisplatin-induced rat nephrotoxicity: the involvement of TLR4/NF- $\kappa$ B signaling pathway. *PLoS One*. 2017;12:e0171612. doi:10.1371/journal.pone.0171612

## Cancer Management and Research

Dovepress

### Publish your work in this journal

Cancer Management and Research is an international, peer-reviewed open access journal focusing on cancer research and the optimal use of preventative and integrated treatment interventions to achieve improved outcomes, enhanced survival and quality of life for the cancer patient.

The manuscript management system is completely online and includes a very quick and fair peer-review system, which is all easy to use. Visit <http://www.dovepress.com/testimonials.php> to read real quotes from published authors.

Submit your manuscript here: <https://www.dovepress.com/cancer-management-and-research-journal>